Site Instrumental de Recherche par Télédétection Atmosphérique

http://sirta.ipsl.polytechnique.fr/

PARISFOG research program

White paper, November 2011

Author: JC. Dupont (IPSL)

With the contributions of
E. Dupont, L. Musson-Genon, K. Sartelet (CEREA)
F. Burnet, L. Gomes (CNRM)
D. Baumgardner (Nat U. Mexico)
D. Jolivet, T. Elias (Hygeos)
M. Haeffelin (IPSL)
D. Khvorostiyanov, L. Menut (LMD)
J. Sciare (LSCE)

Contact: sirtascience@ipsl.polytechnique.fr

Sommaire

1 INTRODUCTION

1.1 Context

[1] Low visibility meteorological conditions, such as fog, are not necessarily considered extreme weather conditions, such as those encountered in storms, but their effects on society can be just as significant. Fog creates situations where our transportation systems on roads, rails, sea and air become more hazardous, requiring specific safety measures to prevent accidents that lead to delays or cancellation of transport. The total economic loss related to fog is comparable with that for tornadoes, even comparable to that for hurricanes or winter storms in some situations [Gultepe et al., 2009]. Fog can form under specific weather back-ground conditions and is also related to local conditions, for example terrain and ecological environments, so fog structures and evolution can differ greatly.

[2] While current numerical weather prediction models are able to forecast situations that are favourable to fog events, these forecasts are usually unable to determine the exact location and time of formation or dissipation. One-dimensional assimilation-forecast models have been implemented at a few airports and provide improved local predictions of fog events, but this approach is limited to locations. The occurrence, development and dissipation of fog result from multiple processes (thermodynamical, radiative, dynamical, and microphysical) that occur simultaneously, through a wide range of conditions, and that feed back on each other inducing non-linear behaviours. This complexity is central to the persistent difficulty associated with providing accurate fog forecasts. Hence to advance our ability to forecast fog processes, we must gain better understanding on how critical physical processes interact with each other, to improve their parametric representations in models.

[3] The present project deals with the better understanding of the multiple processes occurring during the fog life cycle (formation, maintenance and dissipation steps) starting from observations and models means.

1.2 Objectives

[4] The main objectives of our project can be classified into 6 topics, namely observations and algorithms for the technical aspects, and processes (microphysical, chemical, radiative and dynamical) for the scientific aspects.

AEROSOL ASPECTS

(i) **Quantify the role of aerosol properties in regulating cloud condensation nuclei activation during fog events.** Atmospheric aerosols affect climate indirectly through their role as cloud condensation nuclei (CCN) and thereby alter cloud and fog radiative properties. The understanding of the fog and cloud droplet formation potential of aerosols is a requirement for (1) predicting their impacts on fogs and clouds and (2) assessing the uncertainty in climate change predictions.

(ii) **Identify the factor influencing the optical properties of aerosols during the formation and evolution of fog.** Aerosols and fog have an intimate and complex relationship: without aerosols there would be no fog. Fog provides a pathway for changing aerosol properties in multiple ways that change their chemistry, optical characteristics and lifetime.

CHEMICAL ASPECTS

(iii) **Quantify the impact of fog on the Chemistry-transport model CHIMERE.** The project will quantify the impact of taking this process into account by direct comparison to the simulations actually carried out without the impact of the fog effect.

(iv) **Investigate the chemical composition of aerosols during the fog processes.** This study is a perfect case for a better understanding of heterogeneous processes in clouds and offers the advantage to deploy a large set of state-of-the-art instruments to perform real-time chemical mass closure of airborne particles before/after the cloud process as well as the interstitial aerosols & fog droplets.

RADIATIVE – THERMAL ASPECTS

(v) **Explore the question of the aerosol role on fog life cycle, through their radiative impact.** We will study the aerosol implication in the boundary layer radiative budget before the fog formation for infrared flux and also the impact of aerosols and droplets in the fog dissipation by solar radiation heating.

(vi) **Analyse the temporal and vertical variability of temperature gradient** conducting to fog formation. Is there an optimal value? And what is the impact of turbulence and/or aerosol vertical structure on this evolution?

DYNAMICAL ASPECTS

(vii) **Quantify the weight of wind and calculate the critical value of turbulence conducting to the formation and the development of the radiation fog.** We will analyse the balance between the production of liquid water through radiative cooling and drying-out due to turbulence.

(viii) **Better understand the coherent structures in the stable layer close to the ground** just before the fog appearance and **at the top of the fog layer** where radiation cooling tends to form a strong inversion where entrainment and detrainment could be important.

2 STATE OF THE ART

Forecast stake

[5] While the meteorological event is inevitable, there is significant pressure from airport and road transport authorities to obtain more reliable forecasts. Local short-term fog forecasts relying on 1-D assimilation-forecast high resolution models [e.g. Cobel-Isba model; Bergot et al., 2005] have been implemented at airports in Paris, and Lyon, France [Bergot, 2007], and San Francisco, USA [Ivaldi et al., 2006]. These models include precise parameterizations of radiative, turbulent and surface processes, and rely on detailed and continuous near-surface observations of temperature, humidity, wind, radiation and visibility. They produce more accurate fog forecasts than current NWP models [Bergot 2007], but their application remains local. Hence further improvements in fog forecast rely on better understanding of physical processes at stake in the fog life cycle.

Complex interactions

[6] Fog formation results from condensation of water vapour into liquid droplets or ice crystals, as a result of air cooling, moistening and/or through mixing of contrasting air parcels. The most common scenario considered when invoking fog formation over land involves nocturnal radiative cooling under light wind conditions [Roach 1995], while dissipation typically occurs a few hours after sunrise as a result of warming from sensible heat fluxes over a surface heated by solar radiation (the so-called fog burn-off). However, this statement hides a more complex reality, with regions experiencing fog events due to conditions such as advection fog, or stratus lowering rather than the typical radiative fog event [Croft et al. 1997; Tardif and Rasmussen 2007]. Furthermore, the nature and concentration of aerosols present in the surface layer are known to be critical parameters throughout the fog life cycle as their chemical and microphysical properties control the activation process [Rangognio et al., 2009], and their optical properties affect radiative cooling and heating [Elias et al., 2009]. In addition, turbulent mixing is known to be a key but ambiguous factor in influencing fog formation. If turbulent mixing is too low, dew deposition at the surface will inhibit condensation in the atmosphere and hence inhibit fog formation. If turbulence is strong enough, it may promote condensation in a supersaturated surface layer of sufficient depth, and hence lead to fog formation and development [Bergot et al., 2008].

Field campaigns

[7] As reviewed in Gultepe et al. (2007), several field campaigns carried out in Europe and North America have focused on physical and chemical processes involved in continental fog. Early studies revealed that the development of radiation fog results from the balance between radiative cooling and turbulent mixing (e.g. Roach et al. (1976) based on observations performed in Cardington, UK). Other datasets were put together to focus on radiation fog, such as the Fog-82 campaign in Albany, NY USA [Meyer et al., 1986], the Lille-88 and -91 in Northern France [Guédalia and Bergot, 1994] and the Beijing in China [Zhang et al., 2005] field experiments. The role of turbulence was investigated using measurements performed at the Cabauw experimental site in the Netherlands [Duynkerke, 1999]. In the same period, the Po Valley in Northern Italy received considerable attention, with two field campaigns (1989 and 1994) focused on fog microphysical processes and evolution of chemical species [Fuzzi et al., 1992 and 1998].

Fog definition and classification

[8] According to the international definition, fog corresponds to a reduction of horizontal visibility to less than 1000 m due to the existence of water droplets in suspension with the

base touching the surface (AMS Glossary, 2000). A fog event is defined here as the phenomenon during which visibility is lower than 1000 m, but can also include short intervals during which visibility is temporarily slightly higher [Tardif and Rasmussen, 2007].

[9] One of the first classification of fog into types, was made by Willett (1928), later modified by Byers (1959), who identified eleven fog types. There are different kinds of fog classification in the literature and Gultepe et al. (2007) summarized fogs into radiation fog, high-inversion fog, advection–radiation fog, advection fog, and steam fog.

[10] Many factors, for example radiation cooling, warm/cold advection, and precipitation, can affect fog processes. Some fog cases are affected by several factors, but the classification is based on the primary factor that affects fog formation, maturation, and dissipation. Radiation fog is most likely to occur over land [Li, 2001], and usually forms near the surface under clear sky in stagnant air in association with an anticyclone [Gultepe et al., 2007]. So the primary factor for radiation fog is radiative cooling. Two factors affect advection–radiation fog, namely radiative cooling and advection. Advection fog has advection as its dominant factor [Liu et al., 2011]. Precipitation fog forms as raindrops fall into drier air below the cloud; the liquid droplets evaporate to become water vapour, the water vapour cools, and at the dew point it condenses and becomes fog [Tardif and Rasmussen, 2009]

Microphysical processes

[11] Fog drop-size distributions and droplet growth are important features of fog microphysical process. Many studies have illustrated the phenomenon of droplet growth [Eldridge, 1971; Gerber, 1991] showing that multiple processes could be the principal agents of droplet growth. Supersaturated environment [Baronti and Elzweig, 1973], radiative cooling [Roach, 1976], and turbulent mixing [Gerber, 1981] are the most important. However, Choularton et al. (1981) indicated that these processes (radiative cooling, large supersaturation fluctuations, and convective motions) must occur simultaneously to produce larger droplet. Spencer et al. (1976) suggested that the major effect upon the droplet growth process is from the increasing competition for vapour due to the nucleation of new droplets. Intense droplet growth due to water condensation and droplet coagulation was found to lead to bimodal [Podzimek, 1997] or multi-modal [Garcia et al., 2002] drop-size distributions.

[12] Vertical structures of fog droplet size distribution and microphysical property have long been researched, but the results by different researchers are quite controversial. Pilie et al. (1975) found that fog droplet size distributions became narrower and the mean radius decreased with both increasing altitude and increasing age of fog. However, Goodman (1977) and Pinnick et al. (1978) observed opposite features; in all of their cases, the mean droplet diameter and liquid water content increased with height.

Modelling

[13] One-dimensional models are relatively cheaper to run in terms of computational cost, so they have been developed and used widely. Fisher and Gaplan (1963) set up the first fog model, considering vertical diffusion, advection and latent heat. However, this model neglected radiative cooling, large-scale vertical motion and gravitational settling, and the turbulent exchange coefficient was simply calculated as a function of height. Following this, a more sophisticated model was developed by Brown and Roach (1976) including new formulations for turbulence exchange coefficients in the nocturnal boundary layer. A similar model was also used by Musson-Genon (1987) for the quantitative comparison between

computed and observed fog characteristics. Guedalia and Bergot (1994) illustrated in their one-dimensional fog model the importance of advection terms and their role in fog formation and evolution. The major sources of uncertainty for the 1D-models are the assumption of horizontal homogeneity, the not correct representation of clouds, the not properly treated atmospheric turbulence for strongly stable conditions and finally the not adequate fluxes of moisture and heat for heterogeneous surface conditions.

[14] In addition to the one-dimensional models, and due to the complex interactions of various thermodynamical, microphysical and chemical processes, an accurate 3D model is needed [Gultepe et al., 2007]. It accounted for complex topography, turbulent exchange, longwave radiation of surface and atmosphere, shortwave solar radiation, evaporation, condensation, heat budget etc. Wind speed, potential temperature, specific humidity, and the liquid water mixing ratio were predicted by the model. The major sources of uncertainty for the 3D-models are the not sufficient grid resolution near the surface, the difficulties to account for soil and vegetation horizontal heterogeneities and the sensitivity to the model initial conditions.

[15] The coupling of 1-D and 3-D models and their integration with observations lead to promising results for fog forecasting. Bergot et al. (2005) clearly demonstrated the necessity of using surface measurements in 1-D models with a local assimilation scheme.

Radiation fog and dynamical processes

[16] Radiation fog is closely related to radiative cooling and many researchers have attempted to interpret the mechanism of formation for this fog type [e.g., Brown and Roach, 1976; Shi et al., 2005] which has a remarkable diurnal variation, often forming in the light and dissipating after sunrise.

[17] The initial formation of fog appears to depend upon a balance between the production of liquid water through radiative cooling and drying-out due to turbulence [Roach et al., 1976; Zhou and Ferrier, 2008]. Moreover, the influence of turbulence on the liquid water budget decreased with height and was more significant for shallow fogs than for deep fogs. Through numerical simulation, Zhou (1987) found that turbulence inhibited radiation fog formation but was able to promote fog development after its formation. Similarly, Wobrock et al. (1992) found that radiative cooling of the surface and adjacent layer was only able to form shallow and short-term fog, and the formation of high-top and long-duration fog needed additional conditions, such as turbulent mixing and advection. However, the temperature inversion is a vital factor and the inversion migrates above the fog top due to the radiative cooling of the fog top and temperature decreases with height under the fog top inducing a double layer structure with increasing height [Roach et al., 1976; Li et al., 1999]

3 KEY ISSUES

3.1 Interactions between aerosols and fog

3.1.1 Aerosol / droplet observations and data processing

3.1.1.1 Liquid phase and fog droplet at surface level measurement

Contributors: F. Burner (CNRM)

[18] The ground base platform for in situ measurements of the fog microphysical properties that will be deployed during the three field campaigns at SIRTA site between 2010 and 2013 has been recently completed with a Fog-Monitor (FM-100) and a Particulate Volume Monitor (PVM-100) to better characterize the liquid phase.

The FM-100 is an OPC that measures the size spectrum of droplet diameter between 2 and 50µm. The PVM-100 provides a direct measurement of the liquid water content (LWC) and of the extinction (Particle Surface Area) over the same range.

Issues to be addressed

1. Evaluate the closure between FM-100 and PVM measurements: dependence on wind speed and direction? On microphysical properties?
2. Is the overlap between Welas and FM-100 size distribution accurate enough to allow the retrieval of the complete size distribution of wet particles (aerosol and droplet)?
3. Is the measured fog droplet number concentration consistent with the CCN predicted from Köhler (activation closure)?
4. Observed fluctuations of the microphysical properties: what time scales are involved? Link with the other parameters?

3.1.1.2 Dry aerosol at surface level measurement

Contributors: T. Elias (HYGEOS)

[19] In-situ measurements deployed at SIRTA site to document the dry aerosol microphysic and optical properties are composed of a multiple sensors such as one CPC-3025 (total number of particles between 2.5 nm and 2.5µm), one SMPS (particle size distribution between 10.6 and 496nm), one TEOM-FDMS (mass particle in µg/m^3), one aethalometer (black carbon mass at 880nm), one TSI-nephelometer (scattering and back-scattering at 3 wavelengths) and one Grimm-OPC (size distribution between 03 to 2.5µm).

Issues to be addressed

1. Evaluate the particle concentration closure between CPC-3025, SMPS and Grimm-OPC.
2. Evaluate the particle mass closure between SMPS, Grimm-OPC and TEOM-FDMS.
3. Which is the hierarchy in the different classes of dry particles on the optical and radiative closure (nephelometer versus SMPS/Grimm)?

3.1.1.3 Aerosol properties along the vertical

Contributors: M. Haeffelin (IPSL)

[20] SIRTA Observatory gathers vertical profiles of backscatter signal provided by an automatic lidar (named ALS450) at 355nm, a manual lidar (named LNA) at 532 and 1064nm and an automatic ceilometer (named CL31) at 910nm between the ground level and 10, 15 and 7.5 km above ground level (AGL), respectively. Cimel sun-photometer provides total column aerosol optical thickness at 8 wavelengths during the daytime period when solar disk

is visible and surface TSI-nephelometer documents the scattering and backscattering signal at 450, 550 and 700nm.

Issues to be addressed

1. Quantify the vertical profile of hydrated aerosols for mist, quasi-fog and before fog formation.
2. Is there a specific signature of dry or hydrated aerosols characteristic of fog event compared to no-fog event?

3.1.1.4 Fog properties along the vertical

Contributors: J. Delanoë (LATMOS), G. Martucci (NUIG, IE)

[21] FM/CW BASTA cloud radar at 95GHz developed by LATMOS laboratory provides cloud reflectivity and Doppler vertical velocity between 40m and several km AGL. This radar is in development and hard/soft ware will be finalized in a short term period. Cloud radar data are combined with multichannel HATPRO microwave radiometer and lidar backscatter signal to provide input data for multi-module algorithm to derive microphysical structure of fog along the vertical.

Issues to be addressed

1. Evaluate the HATPRO microwave radiometer output concerning the fog liquid water path. Comparison with PVM and FM-100 sensors.
2. What is the spatial and temporal variability of fog droplet microphysic?
3. Which is the optimum technique to derive the fog microphysical and optical structure (Syrsoc, Cloudnet)?

3.1.2 Aerosol processes in fog life cycle

Contributors: J. Delanoë (LATMOS), G. Martucci (NUIG, IE), M. Haeffelin (IPSL), F. Burnet (CNRM), T. Elias (HYGEOS)

[22] **Impact of aerosol on fog.** Aerosols in the atmosphere are composed of organic and inorganic compounds which influence their ability to act as Cloud Condensation Nuclei (CCN): (1) water-soluble inorganic salts and low molecular organic acids are efficient CCN, (2) the effect of organic compounds on cloud droplet activation is still poorly characterized. The ability of aerosol to act as CCN is a strong function of their size, composition and phase state and the CCN activity is adequately modeled by Köhler theory. The critical supersaturation (*Sc*) corresponds to the minimum level of water vapor saturation required to activate a CCN and form a cloud or fog droplet (at a relative humidity above Sc the droplet can spontaneously grow by addition of water).

Issues to be addressed:

1. What is the critical size (dry size) and critical supersaturation, Sc, at which the aerosol becomes a CCN (activation)?
2. What are major sources of fog-active aerosols? What physical/chemical properties dictate fog-forming ability?
3. What is the impact of dry aerosol properties (size, mass) on fog properties (droplet size, liquid water content, sedimentation)?
4. Is there a relationship between the vertical profile of aerosol before fog formation and the fog droplet distribution along the vertical?

[23] **Impact of fog on aerosols.** Fog provides a pathway for changing aerosol properties in multiple ways that change their chemistry, optical characteristics and lifetime. It is likely to have four types of interactions between the aerosol and droplet between pre-fog and post-fog:

(i) No change

(ii) Inertial scavenging, droplet coalescence and sedimentation lead to changes in number and mass concentration and changes in composition.
(iii) Uptake of precursor gases and aqueous processing leads to changes in mass concentration and composition.
(iv) Uptake of water may change aspherical particles to spherical as a result of a liquid layer.

Issues to be addressed:

1. What are the changes in aerosol properties at the surface (size, shape and concentration) before, during and after fog events?
2. Is there a impact of fog on the vertical distribution of aerosols after the fog dissipation?

3.2 *Impact of fog on pollution and chemistry*

3.2.1 Pollution and chemistry observations and data processing

3.2.1.1 Regional pollution heterogeneity

Contributors: L. Menut (LMD)

[24] AirParif measurements in Paris region provide PM2.5 measurement ….

Issues to be addressed

1. What …

3.2.1.2 Boundary layer height

Contributors: M. Haeffelin (IPSL), Y. Morille (LMD)

[25] The high temperature inversions induce very stable conditions favourable for the radiative fog formation. The infrared radiative cooling is responsible for the fog droplet condensation close to the surface, next the development occurs along the vertical. The altitude of the mixing depth (MLD) directly driven by the radiative cooling can be reduced to 100-200m inducing strong concentration in aerosol (potential CCN). The calculation of this mixing layer height is hence critical to understand the vertical extension of fog and to better characterize the properties of the clear sky preceding the fog formation.

Issues to be addressed

1. Is there an optical algorithm to derive the MLD starting from backscatter signal (lidar), turbulence (sodar, radar) or thermodynamical (radiosounding, radiometer) signal? Score? Quality flag?
2. What can be the accuracy of the microwave radiometer for this stable condition? Are we able to detect the temperature inversion? Humidity retrieval? Comparison with in situ measurement.
3. What is the best instrument to detect very stable MLD (lidar, sodar, radar, microwave radiometer)?

3.2.1.3 Chemical measurement

Contributors:J-E. Petit (LSCE), J. Sciare (LSCE)

[26] The LSCE laboratory has deployed an ACSM instrument ……

Issues to be addressed

1. What …

3.2.2 Chemical processes in fog life cycle

Contributors: K. Sartelet (CEREA), L. Menut (LMD), D. Khvorostiyanov (LMD), J. Sciare (LSCE), M. Haeffelin (IPSL), Y. Morille (LMD)

[27] There is growing evidence suggesting that, like sulfate, secondary organic aerosol (SOA) is formed through aqueous-phase reactions in clouds, fogs and aerosols [Altieri et al., 2006]. There is also growing evidence from atmospheric observations that oxalic acid is a product of cloud processing [Heald et al., 2006]. Investigation of the chemical composition of fog processes can be assimilated as a case of study for a better understanding of heterogeneous processes in clouds and offer the advantage to deploy a large set of state-of-the-art instruments to perform real-time chemical mass closure of airborne particles before/after the cloud process as well as the interstitial aerosols & fog droplets. Such studies conducted in the region of Paris will offer extra interest as this region meets contrasted PM chemical composition & physical/optical properties during wintertime [Sciare et al., 2010] including fresh regional emissions (wood burning, traffic) and aged (long range transported) secondary aerosols [Sciare et al., 2011].

[28] The particle concentrations are widely studied for their impact on local air pollution, climate and health. Multiple processes are involved in the emissions, transport and transformations of such particles. Among all the poorly known processes, fog remains difficult to understand and thus predict. It is known however that (radiative) fog can reduce particle concentrations by increasing the wet removal. Also, fog increases vertical mixing and can change the NOx/VOCs chemistry. Globally, fog can change pollutant surface concentrations, but it is unclear to what extent or for what species. To increase the ability of models to better simulate fog and its effects, it is possible to study each process independently or, conversely, to study the overall causes of the fog effects on pollutants.

[29] Comparisons of models and measurements before, during and after fog events will allow us to evaluate how models reproduce the aerosols chemical composition for inorganic and organic components of aerosols and cloud droplets. The evolution of the inorganic fraction before fog events may be modelled using box models such as ISOROPIA (Nenes et al. 1998). During the fog event, the cloud droplet inorganic composition may be estimated using VSRM (Fahey and Pandis, 2003) or a simplified aqueous model (Roustan et al. 2010), and the organic fraction using a model based on Carlton et al. (2008). The comparison model/measurements will focus on inorganic gas and particulate/droplet concentrations, OC mass and SOA properties.

<u>Issues to be addressed:</u>

1. What is the impact of fog on air quality (PM concentrations and composition)?
2. What is the impact of heterogeneous chemistry (during fog events) on SOA formation and on SOA properties (mixing state, volatility, water-solubility, oxidation state)?
3. What is the impact of fog chemical processes on aerosol toxicity (oxy- & nitro-PAH, ROS potential, EC size distribution and mixing state…)?

<u>3.3 Interaction between dynamic and fog</u>

3.3.1 Wind / turbulence observations and data processing

3.3.1.1 <u>Surface level heat fluxes</u>

Contributors: D. Richard (IPGP), post-doc (CEREA)

[30] The latent and sensible heat fluxes are estimated with eddy-covariance methods based on sonic anemometer measurements at 10Hz. Vertical wind speed and humidity fluctuations are combined to derive latent heat, while vertical wind speed and temperature fluctuations are used to derive sensible heat every 5 minutes. SIRTA site has multiple sonic anemometers in zone 1 and zone 4 between 2 and 30m AGL KH20 and LICOR sensors and CSAT3 and GILL 3D sonic anemometer provide humidity variability and wind speed fluctuation, respectively. A scintillometer will be installed at SIRTA site in zone 1 in spring 2012 to estimate heat fluxes.

Issues to be addressed:

1. What is the accuracy of the turbulent heat fluxes derived from eddy-covariance method? Comparisons with the scintillometer retrievals.
2. Is there significant spatial heterogeneity (vertical and horizontal)? Stable conditions especially.
3. What is the order of magnitude of the surface heat fluxes before, during and after fog event?

3.3.1.2 Vertical profiles for clear atmosphere

Contributors: E. Dupont (CEREA), JC. Dupont (IPSL)

[31] Wind and turbulence measurements are composed of a Remtech sodar (wind profile between 100 and 600m), two Leosphere lidars (one short range i.e 40-200m AGL and one long range 100-2000m AGL), a Degréane UHF radar (wind profile between 100 and 2000m AGL), and Metek ultrasonic anemometers (at 10 and 30m AGL). These instruments complement each other in terms of vertical range, and allow retrieving wind profiles between 10 m and about 2000 m. Among the remote sensing instruments, the short range lidar is the more suited to turbulence measurements due to its relatively high sampling rate. In fog situations, the range measurement of the sodar seems to be unaffected while it is reduced for the lidar (to about 100 m for example in the case of 19 February 2011). The abilities of these 2 instruments to characterize turbulence during fog events needs to be further investigated. Statistics and case studies for stable and convective situations will be analysed and the turbulent kinetic energy, sensible and latent heat fluxes will also be estimated and balanced to different fog events, clear-sky events.

Issues to be addressed

1. What relevant information can sodar and lidars provide on the vertical profile of turbulence just before and during fog events?
2. Establish a 3D best product of wind between surface and boundary layer height.
3. What is the typical value of turbulent kinetic energy in the sub-cloud layer and just above the cloud top? Vertical wind speed?
4.
5. Is it possible to use the sodar echo profile to characterise the fog layer, especially to determine its height [Dabas et al., 2011]?

3.3.1.3 Vertical profiles for cloudy atmosphere

Contributors: J. Delanoë (LATMOS, E. Dupont (CEREA)

[32] The new cloud-radar with continuous wave, named BASTA, and developed by the LATMOS, which takes part in the routine observation at the SIRTA site, allows a sampling starting from 20m above the radar (for example 240m for pulsed radar at 95GHz), so dedicated to the studies of fog and low level clouds (high vertical resolution, coherent averaging). However, BASTA is currently optimized in order to improve sensitivity (-40 dBZ at 1 km) and the precipitation / low-level cloud modes (new modes to be added) and to clean

up data above precipitation. This work in progress could be finished at the end of 2011 and BASTA could detect the entire dataset of fog events and so documents their microphysic properties (reflectivity and Doppler, integrated ice content, extinction, particle concentration, droplet size, etc.) but also the dynamic properties (with the Doppler and the restitution of the air vertical speed in the cloudy atmosphere). We will develop the Doppler radar algorithm necessary to derive the fog properties with the radar raw data. The several years of in-situ measurement will be analysed using the concept of normalized distribution developed at the LATMOS laboratory [Delanoë et al., 2005] in order to relate observations and radar retrievals. The method RadOn “reflectivity + Doppler” [Delanoë et al., 2007] and a radar-lidar method [Delanoë and Hogan, 2008] previously developed for the ice clouds, will be applied and adjusted to the properties of the liquid cloud and fog measured during the SIRTA field campaign (ParisFog 2006, 2010-2013). The turbulent kinetic energy dissipation rate, as proposed by Bouniol et al. 2003, will be derived from the temporal variance of the mean Doppler velocity. Sodar is relatively unaffected by fog occurrence and so it can provide accurate profile of 3D component of the wind. Moreover, cup anemometer is not affected by fog formation while the sonic anemometer capacities are reduced.

<u>Issues to be addressed</u>

1. Is it possible to use the sodar echo profile to characterise the fog layer, especially to determine its height [Dabas et al., 2011]?
2. What is the order of magnitude of droplet fall velocity during fog development and fog dissipation? Is there a critical value conducting to fog dissipation?
3. Evaluate vertical wind speed inside fog layer with cloud radar, sodar and sonic anemometer. Temporal variability during fog life cycle.

3.3.2 Dynamic processes in fog life cycle

Contributors: J. Delanoë (LATMOS), E. Dupont (CEREA), L. Musson-Genon (CEREA), JC. Dupont (IPSL), D. Richard (IPGP)

[33] The horizontal heterogeneity of fog events will be analysed with the regional Météo-France stations and the vertical development with the active and passive remote sensing collocated at the SIRTA site. The competitive processes that tend to modulate the fog duration and spatial (vertical and horizontal) development will be analysed. The impact of the near surface turbulence (kinetic energy, sensible and latent heat fluxes) on the horizontal visibility variability during fog event will be studied for radiative and stratus lowering period. The clear atmosphere wind shear effect will be particularly analysed during the vertical development of the fog. The magnitude of sedimentation and precipitation of fog droplets will be will be measured by the BASTA radar when fog develops and when stratus lifts or lowers. The cloud droplet sedimentation proportional to the 6th power of the droplet diameter measures at the surface with the in-situ measurement and inside the stratus cloud with the cloud-radar over the SIRTA site will be (i) validated and (ii) related to the liquid water content and to the fog vertical extension. Consequently, the low limit of the turbulence necessary to condensate water in mixing the wet and cold surface layer for radiative fog will be quantified by comparison between fog and no-fog events [Zhou and Ferrier, 2007].

[34] The period just before the radiative fog formation is characterized by a clear-sky regime defined arbitrarily for visibility larger than 5000m, in contrast to hazy and foggy conditions when visibility can reach dramatically smaller values until 50m. We often note two situations during the clear-sky regime. For the first, we will quantify the impact of the atmospheric boundary layer changes coupled with the solar diurnal cycle. For the second, we will analysis the effect of wind speed, wind direction and humidification near the surface. The starting process of radiation fog formation is the black-body radiative cooling of the ground and the simultaneous convective heat loss in the air adjacent to the ground surface. At a next

stage, the density of the fog is increased so much that the black-body emissivity of the drops becomes effective and the fog takes over a part of the role of cooling medium initially played by the ground.

[35] The stratus lowering process conducting to fog formation is mainly driven by the dynamic [Koracin et al., 2000] at local and regional scale. The mechanism of stratus lowering (thickening) to fog caused entrainment has also been investigated by Oliver et al. (1978). However, important interactions between turbulence, radiation and thermal processes occurred during the stratus-fog transition. We will focus on the variability of the sedimentation and on the intensity of the evaporation rate inside the stratus cloud 3-4 hours before the fog formation. Impact on the vertical gradient of temperature and humidity will be established and compare to previous results [Dupont et al., 2010].

<u>Issues to be addressed:</u>

1. Is there a critical value of turbulence (in terms of TKE, wind speed) conducting to radiative fog formation? Fog development?
2. Are we able to better characterize the coherent structure in the stable layer close to the ground just before the radiative fog formation?
3. What is the level of stability at the top of the fog where entrainment and detrainment are driven by the strong inversion due to fog top radiative cooling?
4. Is there optimum inversion strength conducive to fog formation (balance between radiative cooling, liquid water content, duration, time of formation and dissipation)?

3.4 Interaction between radiation and fog

3.4.1 Radiative / thermal observations and data processing

3.4.1.1 Vertical profiles of temperature

Contributors: JC Dupont (IPSL)

[36] HATPRO microwave radiometer installed at SIRTA site since February 2010 provides a proxy of the vertical of temperature and humidity between the ground level and 10km AGL every 10 minutes. Temperature profile is relatively well document with five independent points between surface and 1km AGL. Only two independent points are available for humidity. To complement the temperature and humidity profiling, SIRTA dataset gathers the twice a day Trappes radiosoundings since 1999. Thermo-hygrometers at 1, 2, 5, 10, 20 and 30m AGL have been installed in October 2011 to precisely document the strong gradients near the surface, especially during nighttime period radiative cooling just before the fog formation. An automatic tethered balloon will be deployed at SIRTA site during the winter 2011-2012, providing temperature and humidity until 300m every 15min. Algorithms will be developed to evaluate each sensor and to calculate a temperature / humidity best product between the surface and the top of boundary layer.

<u>Issues to be addressed</u>

1. What is the ability of HATPRO microwave radiometer to detect and quantify the vertical profile of temperature during stable conditions?
2. Is there a critical value of temperature inversion conducting to mist, quasi fog or fog formation?
3. What is the order of magnitude of the fog top temperature and humidity gradient responsible of turbulent mixing?

3.4.1.2 Radiative measurement at surface level

Contributors: M. Haeffelin (IPSL), JC Dupont (IPSL)

[37] A BSRN radiative flux station is installed at LMD roof (SIRTA zone 2, 15 AGL) since 2003. Shortwave and longwave downwelling fluxes are stored at 1min sampling resolution with a low root mean square error around 5W/m^2 due to ventilated radiometers. Another upwelling and downwelling unventilated radiometers are installed at 30m AGL on the instrumented mast since 2007. Surface radiative budget can be estimated with these last sensors with 10-15 W/m^2 accuracy. Four supplement ventilated radiometers recommended by BSRN network will be installed in November 2011 at 10m AGL in order to measure shortwave and longwave up and downwelling fluxes at 10m AGL. Clear-sky downwelling shortwave and longwave fluxes are calculated flux from Long et al (2006) algorithms. Broadband radiometers are complemented with an infrared radiometer named CLIMAT providing spectral radiation at 8.5, 9.5 and 10.5µm.

Issues to be addressed

1. What are the typical values of longwave radiative cooling conducting to radiative fog formation? And shortwave warming conducting to fog dissipation?
2. Are we able to estimate the impact of hydrated aerosols on longwave radiative cooling?
3. Is there an infrared signature characteristic of mist or fog during hydratation of aerosols 3-4 hours before the fog formation?

3.4.2 Radiative and thermal processes in fog life cycle

Contributors: P. Dubuisson (LOA), M. Haeffelin (IPSL), T. Elias (HYGEOS), JC. Dupont (IPSL)

[38] The radiative fluxes can act either by the shortwave or by the longwave and during the formation, the development and the dissipation of the fog. The interactions between the aerosol/droplet and the solar radiation depend on the particle/droplet properties in scattering, absorbing or reflecting the visible light. On the other hand, the hydrated aerosol and droplet totally modify the interaction between the ground and the atmosphere.

[39] The dry air entrainment at cloud top and the solar absorption effects will be studied at local scale (SIRTA site) and the advective flow impact will be studied at regional scale (Météo-France sites). The impact of solar heating on the liquid water content inside fog directly driven by the absorption coefficient of aerosol is a key process, so the extinction, the absorption and the scattering of the visible radiation by the aerosols will be analyzed [Sandu et al., 2008]. Some sensitivity tests will be made to show the impact of the scattering coefficient of the condensation nuclei and of the fog interstitial aerosol particles on *(i)* the absorption of the solar radiative flux and *(ii)* the infrared radiative cooling at the cloud top. The diurnal effect of solar flux for polluted and clean conditions will be compared and the direct result on the cloud base, cloud top, cloud thickness and liquid water content evaluated with collocated instrument at SIRTA site. The in-cloud modifications due to the solar heating rate induce more turbulence and wind shear and so dry air entrainment at cloud top with important variability range. The vertical wind speed and the wind shear intensity consequences will be investigated by two different methods, namely *closure study* and *sensitivity study*.

[40] The clear-sky regime before the radiative fog formation is characterized by an increase of humidity close to the ground and on the vertical. The aerosol size increases because of hydratation and is detected by lidar remote sensing coupled with the surface in-situ welas measurements. The impact on the longwave fluxes will be calculated by radiative transfer code and measured by pyrgeometer close to the surface.

Issues to be addressed:

1. Are we able to quantify the effect of hydrated aerosol on the infrared cooling before the radiative fog formation? In terms of infrared flux depending on their hygroscopic properties. Is there an impact on the temperature inversion?
2. What is the order of magnitude of the fog top cooling? How the high altitude clouds modulate the infrared cooling at the fog top? What is the impact on the droplet growth and fall velocity?
3. Is there a signature of the aerosol properties on the solar warming within the fog for polluted and clear cases?
4. What is the contribution of the infrared fog top cooling and of the solar warming inside the fog on the vertical development of the fog?
5. Can we quantify the impact of hydrated aerosol on the downwelling longwave flux during the pre-fog event?

4 STRATEGY

[41] We plan to use the synergy between observations and numerical simulations. The observations will be performed at the SIRTA site [Haeffelin et al. 2005] and at regional scale with the Météo-France standard meteorological stations. For ParisFog 2010-2011 and 2011-2012 the most interesting situations will be selected for modelling purpose in order to study key processes identified through data analysis. The modelling will be ensured by the AROME and WRF mesoscale models, the Code_Saturne local scale simulations and the one-dimensional model COBEL.

4.1 Ground observations

4.1.1 Routine measurements at SIRTA

Contributors: C. Pietras (LMD), C. Boitel (LMD)

[42] To provide a dataset suitable to study these processes simultaneously in continental fog, a suite of active and passive remote sensing instruments and in-situ sensors are currently deployed at the SIRTA observatory (http://sirta.ipsl.polytechnique.fr/). SIRTA stands for Site Instrumental de Recherche par Télédétection Atmosphérique. It is a French national atmospheric observatory dedicated to cloud and aerosol research. SIRTA is located in Palaiseau (49N, 2E), 20 km south of Paris (France) in a semi-urban environment. The observatory gathers and operates a suite of state-of-the-art active and passive remote sensing instruments from a large community to document and monitor an ensemble of radiative and dynamic processes in the atmosphere. The detailed description of the state of the atmospheric column is archived and made accessible to the scientific community.

4.1.2 ParisFog Field campaign

Contributors: JC Dupont (IPSL)

[43] The ParisFog field experiment (http://sirta.ipsl.polytechnique.fr/parisfog/) was designed to shed some light on these questions by (1) monitoring simultaneously all important processes and (2) sampling a large range of conditions during four 6-month winter seasons (Oct. 2006 – Mar. 2007, October to March 2010, 2011, 2012, 2013). To do so, the experimental setup was designed to monitor on a routine basis surface conditions, large and small-scale dynamics, radiation, turbulence, precipitation, droplet and aerosol microphysics, and aerosol chemistry, combining in-situ and remote sensing instruments on a long-term basis to describe the complete environment in which fog develops. The long observing period was intended to sample processes taking place during contrasting scenarios, such as fog formation versus non-formation in similar conditions (quasi-fog), formation in clean and polluted air masses, and evolution of different fog types.

[44] A 6-month field campaign like this requires efforts to automate measurements and a significant part of the SIRTA team was to ensure this work. Automatic and real-time quick-looks of major part of the instruments are available on the ParisFog public web page (http://sirta.ipsl.polytechnique.fr/parisfog/donnees/3.html). The level one dataset is available in private access. This dataset accounts for a unique format for the header and for the time (1min, 5min or 1hour sampling), which permit us to quick analyse multiple data sensors.

[45] The ParisFog 2010-2011 is focused on droplet and aerosol microphysic (size distribution between 4 nm and 50µm, liquid water content, black carbon, PM2.5) and on near surface dynamic (vertical profile between surface and the top of boundary layer height).

[46] For the ParisFog 2011-2012, we have completed the droplet microphysic instruments in adding a TSI nephelometer (scattering and backscattering of in-situ aerosols at three wavelengths) and a second welas sensor. Temperature and humidity sensors are also installed at 1, 2, 5, 10, 20 and 30m to precisely document the thermal structure of the atmosphere close to the surface. Finally, a TPS-3100 Hotplate precipitation sensor allows us to measure the very low precipitation rate smaller than 0.5mm/hr. A tethered balloon in order to measure vertical profiles of temperature and humidity at the high repetition rate of 3 or 4 per hour between the surface and 300m high is deployed during specific period when strong fog forecast occurred.

4.1.3 Regional measurement with MétéoFrance stations

Contributors: JC. Dupont (IPSL), M. Haeffelin (IPSL)

[47] The Météo-France standard meteorological stations provide surface parameters such as temperature, relative humidity, atmospheric pressure, precipitation rate at 2 m AGL (Above Ground Level) and wind speed and direction at 10 m AGL. A 10-years dataset is available with 1 hour temporal sampling concerning for each station. The local and regional heterogeneities and the representativity of each site will be estimated.

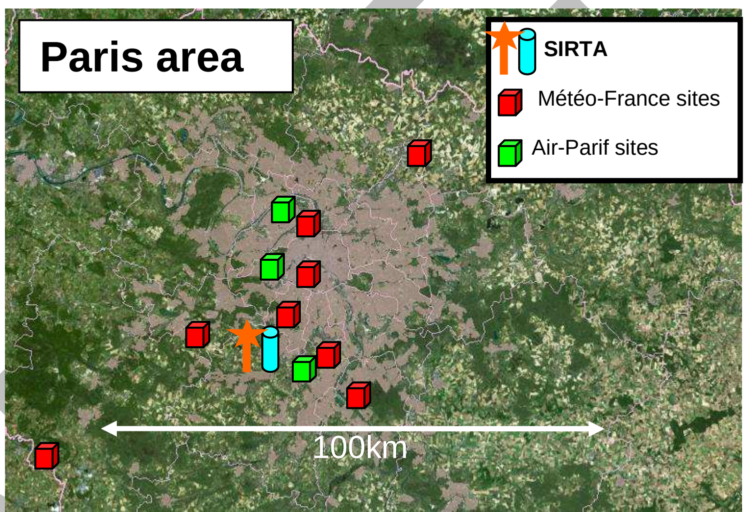

Figure 1 : Météo-France and Air-Parif sites in Paris area considered in this project.

[48] The major part of the data is already stored in the SIRTA database and the table 1 shows the chronology of all the data: routine SIRTA observations, intensive period with additional instruments and Météo-France sites for surface standard meteorological data (temperature, humidity, wind speed and direction, pressure, precipitation, visibility, etc). So, the project is based on existing data and the risk is very limited.

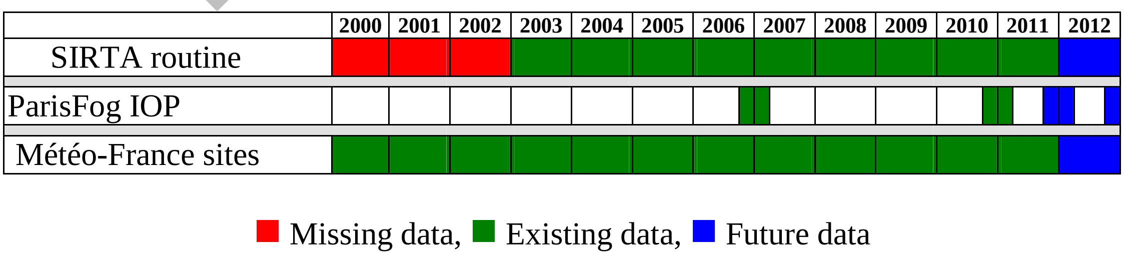

Table 1. Availability of the routine SIRTA observations, ParisFog intensive period and Météo-France site data.

[49] The time sampling for Meétéo-France sites is 1hour and 1min for the SIRTA site. The current methodology to consider a fog event is to use the 10min average horizontal visibility and to have 3 time steps with visibility smaller than 1000m during 5 time steps [Tardif and Rasmussen, 2007]. We will compare the probability statistic distribution of the 1min, 10min and 1 hour visibility data at the SIRTA site. Next, we will develop a new criterion starting from this 1hour data in order to be homogenous with some others studies [Witiw and LaDochy, 2008]. The heterogeneity of some fog characteristics inside the Paris area will be analysed such as the occurrence, the duration, the start and end time, the type of fog (radiative, stratus lowering, etc.). The spatial extension will also be quantified to show if the horizontal extension is very local or if the fog owns a regional coverage. In the same time, the methodology will be applied to quasi-fog and near fog event to be able to consider a more significant dataset with a visibility a little bit more important.

4.2 Spatial observations

Contributors: T. Elias (HYGEOS), D. Jolivet (HYGEOS)

[50] High variability of sources, transport processes and atmospheric conditions causes a strong horizontal heterogeneity of aerosol fields and fog occurrence, which can be resolved by satellite instruments in complement to surface networks. Satellite data processing algorithms are developed to extract information exclusively on aerosols or on fog, with mist being usually disregarded as a transition event between dry aerosols and fog droplets. However, mist has a significant impact on radiative budget at surface level and on the whole atmospheric column.

[51] Mist is composed of aerosols taking up water when ambient relative humidity increases larger than 80%. Consequently aerosol grows and aerosol extinction is multiplied by a factor from 5 to 20, increasing significantly the aerosol direct effect. It is furthermore an important component of the fog life cycle, as providing the initial conditions of radiative fog formation, and hydrated aerosols affecting the dissipation conditions, as they remain present in the fog as interstitial aerosols. Mist is also observed even when the fog does not form, the cumulated mist duration in a season being ten times longer than fog duration. Mist is observed almost 1000 hours at SIRTA during the 2010-2011 seasons.

[52] We will study how to provide information on mist from satellite observation. Low cloud detection is provided by the EUMETSAT/SAF NWC (Satellite Application Facility, Now Casting) project, but not distinguishing between fog and low stratus. One objective of the PreViBOSS (Prévision de la Visibilité dans le cycle de vie du Brouillard par Observation Sol et Satellite) project is to evaluate this product in terms of surface parameters, as relative humidity, visibility, cloud base height, and to evaluate the proportion of fog presence over all low cloud detected cases. We will identify what typology is given by the SAF NWC product when mist is present at SIRTA. Besides, the algorithm dedicated to aerosol may screen out mist situations as "cloudy". The SMAOL algorithm (SEVIRI/MSG to Monitor Aerosol Over Land) will be extended beyond the "clear-sky" pixels to derive the aerosol optical thickness and also extrapolate surface visibility in mist. SEVIRI/MSG data will be processed for the high temporal resolution adapted to study the impact of changing relative humidity on aerosol optical properties.

4.3 Modelling

[53] By using mesoscale, local and one-dimensional models, we plan to better understand the key processes during the different steps of the fog life cycle: coupling between radiation and dynamic, impact of aerosol properties on fog droplets, role of the chemistry on fog formation, etc. Moreover, the parameterizations include in the mesoscale model will be tested and possible improvement could be suggested.

4.3.1 1D-model coupled with WRF

Contributors: S. Stolaki (LMD Post-Doc)

[54] A one-dimensional model will be run at SIRTA site (LMD post-doc, 10/2011-10-2012) to make sensitivity test on each process impacting the fog life cycle. A first step consists in selecting a very well documented case study of radiative fog in order to evaluate the 1D-model outputs. The weight of each parameter could be changed and the role of each process calculated. The choice of the 1D-model will be discussed (COBEL, PAFOG, Code_Saturne 1D, Meso-NH 1D, etc.).

4.3.2 Radiative transfer code

Contributors: P. Dubuisson (LOA)

[55]

4.3.3 Code_Saturne and Polair3D/Polyphemus

Contributors: L.Musson Genon, K. Sartelet (CEREA)

[56]A first version of Code_Saturne adapted to fog simulation has been developed during the PhD thesis of X. Zhang. The 1-D version will be used to simulate new interesting situations and some comparisons with other 1-D models will be carried out.

[57] Code_Saturne will be completed in order to take into account gas (CB5 ; RACM2) and aerosols (SIREAM and MAM). Further developments will be conducted in order to compute cloud droplet composition, as detailed in paragraph 3.3.3. In other respects, a detailed land use coverage description including building, forest area treated with porosity technique, grass and water surface is now implemented in the code (Zaidi at al., 2011). A 3-D version will be used to study the effects of local heterogeneities during some specific events. Special focus will be addressed on coupling aerosols and fog droplet nucleation schemes, 3d radiation including absorption and diffusion processes and its interactions with turbulence and fog structure. For chemical boundary conditions, Code_Saturne will use concentrations from the three-dimensional chemistry transport model Polair3d of the air quality modelling platform Polyphemus (Sartelet et al. 2007a, 2007b; Royer et al. 2011). To simulate Greater Paris regional air quality, Polair3d/Polyphemus will use meteorological fields from WRF and emission inventories from AIRPARIF. The simulation will be evaluated using AIRPARIF measurements of O_3, NO, NO_2, PM_{10} and $PM_{2.5}$, and SIRTA measurements of inorganic gas and aerosol composition, OC mass and SOA properties. A comparison of Polair3d/Polyphemus and Code_Saturne (1D or 3D) simulations will allow us to better understand the role of the local meteorological dynamics on the chemical composition of particles and cloud droplets during fog events.

4.3.4 AROME

Contributors: Y. Seity (CNRM)

[58] The mesoscale model AROME [Seity el al., 2011] will be evaluated at the regional and the local scale. The 2010/2011 winter period will be simulated with the most recent operational version of AROME used at Météo-France at 2.5km horizontal resolution and 60 vertical levels (15 levels below 1 km and a lowest model level at 10m) over a regional domain covering the Paris area. Initial and lateral conditions will be taken from the operational AROME analyses based on a 3D-Var assimilation cycle using a wide range of observations. Some additional experiments will be performed at higher spatial resolution (horizontal and vertical) and possible with some modifications in physics (microphysics, radiation, etc.). The settings of these additional experiments will be determined by an on-going one-dimensional comparison between AROME and the COBEL system [Bergot, 2007] performed over the Roissy airport.

4.3.5 WRF

Contributors: D. Khvorostiyanov (LMD)

[59] The fog occurrence, the time delay, the fog duration and the heterogeneity at regional scale between the WRF fog modelling and surface observations will be quantified. When the observations indicate fog and WRF indicates no-fog, we will try to identify the thermodynamical and radiative variables that induce a wrong formation of fog. Is It specific at one site? What is the order of magnitude of this lack of information (0.01°C or 1°C, 0.5% or 2% for the relative humidity)? We will also quantify the impact of this wrong formation of the thermodynamical variables at regional scale to show if a very local fog event (observed only on one site, i.e 2x2km for WRF) is likely to modify the entire region (i.e 50x50km).

[60] The first fog diagnostics with WRF is to estimate the liquid water content in the surface layer. Being a threshold process, if fog is not diagnosed but observed, an additional diagnostic has to be done. This second fog diagnostic is based on two concepts: (1) the presence of fog induces typical thermodynamical absolute values such as relative humidity or wind speed and (2) the initial phase, 3-4 hours before the fog formation, owns specific characteristics in terms of time evolution of infrared cooling or vertical gradient of temperature/humidity. By directly comparing the two regional simulations (with and without fog), the spatial extension of the fog will be analyzed as well as the horizontal heterogeneity of fog. The impact of fog will be studied in terms of its spatial extent on the region and its interactions with neighbouring areas after transport.

[61] This second evaluation of the simulated fog will be more local and over the SIRTA site where specific measurements were made. The characteristics of the boundary layer, such as the vertical extension, are significantly influenced by fog formation. Two WRF simulations will be compared in terms of the vertical structure of the surface and boundary layer. In order to quantify the model accuracy, the diagnosed boundary layer height (BLH) will be compared to the BLH diagnosed using the STRAT algorithm [Morille et al., 2007] applied on the SIRTA lidar backscatter signal vertical profiles.

4.3.6 CHIMERE

Contributors: L. Menut (LMD)

[62] After the quantification of the vertical changes (over the SIRTA) and the horizontal changes (over the Paris area) induced by fog modelling with WRF, these two meteorological model configurations will be used to simulate the Paris area atmospheric composition using the CHIMERE chemistry-transport model. For pollutants concentrations, the condensate liquid water can totally modify the mixing ratio and so the chemistry nears the surface. Variations in the atmospheric liquid water content in WRF simulation can lead to large differences in PM10 concentrations [De Meij et al., 2009], in particular via the SO2 oxidation by cloud or fog [Faust et al., 1993] hydrogen pyroxide. In the presence of fog, the diurnal

cycle of the mixing layer is altered (by perturbing the convection cycle, the surface heat and latent fluxes, the BLH) and so the interactions between the pollutants and liquid water are enhanced. The impact of fog on surface concentrations will be evaluated using the AIRPARIF measurements over the whole Paris area by comparing observed and modelled hourly surface concentrations of NO, NO2 and PM10. Using the SIRTA measurements, a finer comparison will be made by comparing the vertical structure of the atmosphere and the size distribution of the surface aerosols.

5 Annexes

5.1 *Observations at SIRTA site*

Water vapor

Instrument	Network	Type[1]	Time[2]	Laboratory	PI
Hygrometer		Surface	Routine	LMD	C. Pietras
Microwave radiometer *Hatpro*	MWRNET	Integrated, profile	Routine	LMD	JC. Dupont
Microwave radiometer *Drakkar*		Integrated	Routine	LATMOS	C. Legac
GPS	RGP IGN	Integrated	Routine	LMD	JC. Dupont
Sun-photometer	PHOTON	Integrated	Routine	LOA	P. Goloub
Radiosoundings	MétéoFrance	Profile	Routine (2 times a day at Trappes)	DSO/DOA	F. Besson

Liquid water / solid and precipitations

Instrument	Network	Type	Time	Laboratory	PI
LIQUID WATER (microphysic – effective radius, size distribution, concentration and LWP)					
Hygrometer		Soil	Routine	LMD	JC. Dupont
Fog Monitor (FM-100)		Surface	IOP ParisFog	CNRM	F. Burnet
PVM Gerber		Surface	IOP ParisFog	CNRM	F. Burnet
Palas Welas		Surface	IOP ParisFog	LRPC	F. Morange
Palas Welas		Surface	IOP ParisFog	CNRM	F. Burnet
Microwave radiometer *Hatpro*	MWRNET	Integrated, Profile	Routine	LMD	JC. Dupont
Microwave radiometer *Drakkar*		Integrated	Routine	LATMOS	C. Legac
LIQUID WATER (macrophysic – base and top altitude, cloud fraction, optical thickness**)**					
Backscatter lidar *LNA, ALS450*	CLOUDNET	Profile	Routine	LMD	C. Pietras
Cloud radar (95 GHz) *BASTA, RASTA*	CLOUDNET	Profile	Routine	LATMOS	J. Delanöe
Visible imager *TSI*		Integrated	Routine	LMD	JC. Dupont
ICE WATER (shape, size distribution)					
Backscatter lidar *LNA, ALS450*	CLOUDNET	Profile	Routine	LMD	C. Pietras
Infrared radiometer *CLIMAT*		Integrated	Routine	LOA	G. Brogniez
PRECIPITATIONS					
Hotplate Yes TPS3100		Surface	Routine	LMD	J-C. Dupont
Spectro-pluviometer		Surface	Routine	LATMOS	N. Powell
Rain gauge 3030-3029		Surface	Routine	LMD/CEREA	C. Pietras E. Dupont
Picarro		Surface	Routine	LSCE	F. Vimeux

[1] We consider 4 types of measurements: soil (inside the ground between -5 and -50cm), at the surface (between 2 and 30m), per profile (between 40m and a few km) and integrated (sum on the total column).
[2] We consider 2 types of measurements : routine (automatic mode or manual but during several years et IOP (between several days and several months)

AEROSOLS

Instrument	Network	Type	Time	Laboratory	PI
Microphysic – size distribution, effective radius, concentration, mass, optical thickness					
SMPS		Surface	IOP ParisFog	CNRM	L. Gomes
CPC		Surface	IOP ParisFog	CNRM	L. Gomes
CCNC-100		Surface	IOP ParisFog	CNRM	G. Roberts
Aethalometer		Surface	IOP ParisFog	LSCE	J. Sciare
TEOM-FMDS		Surface	IOP ParisFog	LSCE	J. Sciare
Grimm-OPC		Surface	IOP ParisFog	LSCE	J. Sciare
TSI nephelometer		Surface	IOP ParisFog	LISA	P. Formenti
Sun-photometer	PHOTON	Integrated	Routine	LOA	P. Goloub
Macrophysic – base and top altitude, geometrical thickness					
Backscatter lidar *LNA, ALS450*	EARLINET	Profile	Routine	LMD	C. Pietras

RADIATIVE FLUXES

Instrument	Network	Type	Time	Laboratory	PI
Broadband radiometers (UV, Vis, IR) *Downwelling, clear-sky*	BSRN	Surface	Routine	LMD	M. Haeffelin
Broadband radiometer (Vis, IR) *Up and Downwelling*		Surface	Routine	CEREA	E. Dupont

HEAT FLUXES

Instrument	Network	Type	Time	Laboratory	PI
Sensible heat flux		Surface	Routine	LMD CEREA	JC. Dupont E. Dupont
Latent heat flux		Surface	Routine	LMD IPGP	JC. Dupont D. Richard
Turbulent fluxes		Surface	Routine	LMD CEREA	JC. Dupont E. Dupont

THERMODYNAMIC

Instrument	Network	Type	Time	Laboratory	PI
THERMIC					
Thermometer		Surface	Routine	LMD CEREA	JC. Dupont E. Dupont
Thermometer		Surface 1, 2, 5, 10, 20, 30m	Routine	IPGP	D. Richard
Thermometer		Surface 1, 2, 4, 7, 10m	Routine	LMD	JC. Dupont
Microwave radiometer *Hatpro*	MWRNET	Profile	Routine	LMD	JC. Dupont
Radiosounding	Météo-France	Profile	Routine (2 times a day at Trappes)	DSO/DOA	F. Besson
DYNAMIC (wind speed and direction, turbulent kinetic energy)					
Cup anemometer		Surface	Routine	LMD IPGP	JC. Dupont D. Richard
Sonic anemometer		Surface	Routine	LMD CEREA IPGP	JC. Dupont E. Dupont D. Richard
PA2 Sodar		Profile	Routine	CEREA	E. Dupont

UHF Radar		Profile	Routine	CEREA	E. Dupont
Doppler Lidar (WLS7, low range)		Profile	Routine	CEREA	E. Dupont
Doppler Lidar (WLS70, high range)		Profile	Routine	CEREA	E. Dupont
Radiosounding	MétéoFrance	Profile	Routine (2 times a daya t Trappes)	DSO/DOA	F. Besson

5.2 References

Baronti, P., and E lzweig, S. (1973), A Study of Droplet Spectra in Fogs, Journal of the Atmospheric Sciences 30(5), 903-908.

Bergot T., Carrer D., Noilhan J., Bougeault P. (2005), Improved site-specific numerical prediction of fog and low clouds: A feasibility study, *Weather and Forecasting*, *20*, 627–646.

Bergot, T., **M. Haeffelin**, **L. Musson-Genon**, R. Tardif, M. Colomb, **C. Boitel**, G. Bouhours, T. Bourriane, T. Elias, et al., Paris-FOG: des chercheurs dans le brouillard, *La Météorologie, 62*, 2008.

Brown, R. and Roach, W. T.: The physics of radiation fog, Part II: A numerical study, Q. J. Roy. Meteor. Soc., 102, 335–354, 1976.

Byers, H.R. (1959), General Meteorology, Third Ed., (McGraw Hill, New York 1959)

Carlton, A.G., Turpin, B.J., Altieri, K.E., Seitzinger, S.P., Mathur, R., Roselle, S.J., and Weber, R.J. (2008), CMAQ model performance enhanced when in-cloud secondary organic aerosol is included: comparisons of organic carbon predictions with measurements, Environ. Sci. Technol., 42, 8798-8802.

Choularton, T.W., Fullarton, G., Latham, J., Mill, C.S., Smith, M.H., and Stromberg, I.M. (1981), A field study of radiation fog in Meppen, West Germany, Quart. J. Roy. Meteor. Soc. 107, 381–394.

Croft, P.J., Pfost, R.L., Medlin J.M., and Johnson, G.A. (1997), Fog forecasting for the Southern Region: A conceptual model approach, Weather and Forecasting 12, 545–556.

Dabas, A., S. Remy, T. Bergot (2011), Use of a Sodar to Improve the Forecast of Fogs and Low Clouds on Airports, Pure and Applied Geophysics, DOI 10.1007/s00024-011-0334-y

De Meij A., Gzella, A., Cuvelier, C., Thunis, P., Bessagnet, B., Vinuesa, J.F., **Menut, L.**, Kelder H., 2009, The impact of MM5 and WRF meteorology over complex terrain on CHIMERE model calculations. , Atmos. Chem. Phys., 9, 6611-6632

Duynkerke, P. G. (1999), Turbulence, radiation and fog in Dutch stable boundary layers, *Bound.-Layer Meteor.*, *90*, 447–477.

Eldridge, R.G. (1971), The relationship between visibility and liquid water content of fog, J. Atmos. Sci. 28, 1183–1186.

Elias, T., **M. Haeffelin**, **P. Drobinski**, **L. Gomes**, J. Rangognio, **T. Bergot**, P. Chazette, J.-C. Raut, and M. Colomb (2009), Particulate contribution to extinction of visible radiation: pollution, haze, and fog, *Atm. Res*., doi:10.1016/j.atmosres.2009.01.006.

Fahey, K.M. and Pandis, S.N. (2003) Size-resolved aqueous-phase chemistry in a three-dimensional chemical transport model}, J. Geophys. Res., 108, 4690, doi:10.1029/2003JD003564.

Fisher, E. L. and Caplan, P.: An experiment in the numerical prediction of fog and stratus, J. Atmos. Sci., 20, 425–437, 1963.

Fuzzi, S., Facchini M.C., Orsi G., Lind J.A., Wobrock W., Kessel M., Maser, R., Jaeschke W., Enderle K.H., Arends B.G.,, Berner, A., Solly A., Kruisz C., Reischl G., Pahl S., Kaminski U., Winkler P., Ogren J.A., Noone K.J., Hallberg, A., Fierlinger-Oberlinninger H., Puxbaum H., Marzorati A., Hansson H.-C., Wiedensohler A., Svenningsson I.B., Martinsson B.G., Schell D., and Georgii H.W. (1992), The Po Valley Fog Experiment 1989. An Overview, *Tellus, 44B*, 448-468.

Fuzzi, S., Laj, P., Ricci, L., Orsi, G., Heintzenberg, J., Wendisch, M., Yuskiewicz, B., Mertes, S., Orsini, D., Schwanz, M., Wiedensohler, A., Stratmann, F., Berg, O.H., Swietlicki, E., rank, G., Martinson, B.G., Günther, A., Diersen, J.P., Schell, D., Jaeschke, W., Berner, A., Dusek, U., Galambos, Z., Kruisz, C., Mesfin, N.S., Wowbrock, W., Arends, B., and Ten B.H., (1998), Overview of the Po Valley fog experiment 1994 (CHEMDROP), Contr. Atmos. Phys. 71, 3–19.

Garcia-Garcia, F., Virafuentes, U., and Montero-Martinez, G. (2002), Fine-scale measurements of fog-droplet concentrations: A preliminary assessment, Atmos. Res. 64, 179–189.

Gerber, H.E. (1981), Microstructure of a radiation fog, J. Atmos. Sci. 38, 454–458.

Gerber, H. (1991), Supersaturation and droplet spectral evolution in fog, J. Atmos. Sci. 48, 2569–2588.

Goodman , J. (1977), The Microstructure of California Coastal Fog and Stratus, Journal of Applied Meteorology 16(10), 1056-1067.

Guedalia, D. and Bergot, T. (1994), Numerical forecasting of radiation fog. Part II: A comparison of model simulations with several observed fog events, Monthly Weather Rev. 122, 1231–1246.

Gultepe I., Tardif R., Michaelides S.C., Cermak J., Bott A., Bendix J., Müller M. D., Pagowski M., Hansen B., Ellrod G., Jacobs W., Toth G., Cober S. G. (2007), Fog research: A review of past achievements and Future perspectives, *Pure and Applied Geophysics*, *164*, 1121-1159

Gultepe, I,.Pearson, G., Milbrandt, J. A., Hansen , B., Platnick, S., Taylor , P., Gordon , M., Oakley, J. P., and Cober, S. (2009), the Fog Remote Sensing and Modeling Field Project, Bulletin of the American Meteorological Society 90, 341-359.

Haeffelin, M., T. Bergot, T. Elias, R. Tardif, D. Carrer, P. Chazette, M. Colomb, **P. Drobinski**, E. Dupont, **J-C. Dupont**, L. Gomes, L. Musson-Genon, **C. Pietras**, A. Plana-Fattori**, A. Protat**, J. Rangognio, J-C. Raut, S. Rémy, D. Richard, J. Sciare, and X. Zhang (2008), PARISFOG, shedding new light on fog physical processes, *Bull. Amer. Meteor. Soc.*.

Haeffelin, M., L. Barthès, O. Bock, **C. Boitel**, S. Bony, D. Bouniol, H. Chepfer, M. Chiriaco, J. Cuesta, **J. Delanoë**, **P. Drobinski**, J-L. Dufresne, C. Flamant, M. Grall, A. Hodzic, F. Hourdin, F. **Lapouge**, Y. Lemaître, A. Mathieu, **Y. Morille**, C. Naud, V. Noël, B. O'Hirok, J. Pelon, **C. Pietras**, **A. Protat**, B. Romand, G. Scialom, and R. Vautard (2005), SIRTA, a ground-based atmospheric observatory for cloud and aerosol research, *Annales Geophysicae*, *23*, 253-275.

Koracin D., Lewis J., Thompson W. T., Dorman C. E., Businger J. A. (2001), Transition of stratus into fog along the California Coast: Observations and modeling, *J. Atmos. Sci. 58*, 1714–1731.

Li , Z.H., Huang, J.P., Zhou , Y.Q., and Zhu , S.W. (1999), Physical structures of the five-day sustained fog around Nanjing in 1996, Acta Meteorologica Sinica 57, 622-631. (In Chinese)

Liu, D.Y., S. J. Niu, J. Yang, L. J. Zhao, J. J. Lu, C. S. Lu (2011), Summary of a 4-Year Fog Field Study in Northern Nanjing, Part 1: Fog Boundary Layer, Pure and Applied Geophysics, DOI 10.1007/s00024-011-0343-x

Meyer M. B. and G. Garland LaLa (1989), Climatological aspects of radiation fog occurrence at Albany, New York, *Journal of Climate, 3*, 577-586

Menut L. and B. Bessagnet, 2010, Atmospheric composition forecasting in Europe, *Annales Geophysicae*, *28*, 61-74

Morille Y., **M. Haeffelin**, **P. Drobinski**, and J. Pelon (2007), STRAT: An automated algorithm to retrieve the vertical structure of the atmosphere from single-channel lidar data, *J. Atmos. Oceanic Technol.*, *24*, 761– 775, doi:10.1175/JTECH2008.1.

Musson-Genon, L. (1987), Numerical simulation of a fog event with one-dimensional boundary layer model, *Mon. Wea. Rev., 115*, 592-607.

Nenes, A., Pandis, S.N., and Pilinis, C. (1998), {ISORROPIA: A new Thermodynamic Equilibrium Model for Multicomponent Inorganic Aerosols, Aquatic geochemistry, 4, 123-152.

Oliver D. A., Lewellen W. S., Williamson G.G. (1978), The Interaction between Turbulent and Radiative Transport in the Development of Fog and Low-Level Stratus, *J. Atmos. Sci.*, *35*, 301–316

Pilié R.J., Mack E.J., Kocmond W.C., Rogers C.W., Eadie W.J. (1975), The life cycle of valley fog. Part I: Micrometeorological characteristics, *J. Appl. Meteor.*, *14*, 347–363.

Pinnick, R.G., Hoihjelle, D.L., Fernandez, G., Stenmark, E.B., Lindberg, J.D., and Hoidale, G.B. (1978), Vertical structure in atmospheric fog and haze and its effects on visible and infrared extinction, *J. Atmos. Sci.* 35, 2020–2032.

Podzimek , J. (1997), Droplet Concentration and Size Distribution in Haze and Fog, *Studia Geoph. et Geod*. 41, 277-296.

Roach , W. T. (1976), On the effect of radiative exchange on the growth by condensation of a cloud or fog droplet, *Quarterly Journal of the Royal Meteorological Society* 102 (432), 361-372

Roach, W.T. (1995a), Back to basics: Fog: Part 2 – The formation and dissipation of land fog, *Weather* 50, 7–11.

Roustan Y., **Sartelet K.**., Tombette M., Debry É. and Sportisse B. (2010) Simulation of aerosols and gas-phase species over Europe with the POLYPHEMUS system. Part II: Model sensitivity analysis for 2001. Atmos. Env., 44 (34), p4219-4229, doi:10.1016/j.atmosenv.2010.07.005.

Royer P., Chazette P., **Sartelet, K**., Zhang Q.J., Beekmann M. and Raut J.-C. (2011) Lidar-derived PM10 and comparison with regional modeling in the frame of the MEGAPOLI Paris summer campaign. Atmos. Chem. Phys. Discuss., 11, 11861-11909, accepté pour publication dans ACP.

Sartelet K., Debry E., Fahey K., Roustan Y., Tombette M., Sportisse B. (2007a) Simulation of aerosols and gas-phase species over Europe with the Polyphemus system. Part I: model-to-data comparison for 2001. Atmos. Env., 41 (29), p6116-6131, doi:10.1016/j.atmosenv.2007.04.024.

Sartelet K., Hayami H. and Sportisse B. (2007b) Dominant aerosol processes during high-pollution episodes over Greater Tokyo. J. Geophys. Res., 112, D14214, doi:10.1029/2006JD007885.

Seity Y., P. Brousseau, S. Malardel, G. Hello, P. Bénard, F. Bouttier, C. Lac, V. Masson: The AROME-France convective scale operational model, *Monthly Weather Review*, 2011. doi: 10.1175/2010MWR3425.1

Shi, H., H. Wang, L. Qi, and J. Bai, 2005: Numerical simulation of radiation fog event in Yangtze River. Journal of PLA University of Science and Technology (Natural Science), 6(4), 404–408. (in Chinese)

Tag P. M. and Peak, J. E. (1996), Machine learning of maritime fog forecast rules, *J. Appl. Meteor., 35*, 714–724.

Tardif R. (2007), The impact of vertical resolution in the explicit numerical forecasting of radiation fog: A case study, *Pure Appl. Geophys., 164*, 1221-1240

Tardif, R. and R. M. Rasmussen (2007), Event-based climatology of fog in the New York City region, *J. Appl. Meteor. Climatol.*, *46*, 1141-1167.

Telford, J., and S. K. Chai (1984), Inversions and fog, stratus and cumulus formation in warm air over cooler water, *Bound. Layer Meteor., 29*, 109–137.

Valari M. and **L. Menut**, 2008, Does increase in air quality models resolution bring surface ozone concentrations closer to reality?, Journal of Atmospheric and Oceanic Technology, DOI: 10.1175/2008JTECHA1123.1

Van der Welde, I. R., G. J. Steeneveld, B. G. J. Wichers Schreur, A. A. M. Holtslag (2010), Modeling and forecasting the onset and duration of severe radiation fog under frost conditions, *Monthly Weather Review*, *138*, 4237-4253.

Willet, H.C. (1928), Fog and haze, their causes, distribution, and forecasting, Monthly Weather Rev. 56, 435–468.

Wobrock, W., and Coauthors, 1992: Meteorological characteristics of the Po Valley fog. Tellus, 44B, 469–488.

Zaîdi, H., **Dupont E.**, Milliez, M., Carissimo, B., **Musson Genon, L.**, 2011: Numerical simulations of the atmospheric flow at microsacle over a complex site using an atmospheric CFD code, submitted to *Bound.-Layer Meteor.*

Zhang , G.Z, Bian , L.G., Wang , J.Z., Yang , Y.Q., Yao , W.Q., and Xu , X.D. (2005), The boundary layer characteristics in the heavy fog formation process over Beijing and its adjacent areas, Science in China Series D (Earth Sciences) 48, suppl. 2, 88-101.

Zhou, B., 1987: The numerical modeling of radiation fog. Acta Meteorologica Sinica, 45(1), 21–29. (in Chinese)